Synthesis, structure and magnetic properties of a trinuclear [$Mn^{III}Mn^{II}_2$] single-molecule magnet

Richard T. W. Scott,[a] Simon Parsons,[a] Muralee Murugesu,[b] Wolfgang Wernsdorfer,[c] George Christou[b] and Euan K. Brechin*[a]

Received (in Cambridge, UK) 1st February 2005, Accepted 1st March 2005
First published as an Advance Article on the web 15th March 2005
DOI: 10.1039/b501504a

Ferromagnetic exchange between the three Mn ions in the complex [$Mn_3(Hcht)_2(bpy)_4](ClO_4)_3$ leads to a spin ground state of $S = 7$; single crystal studies reveal the temperature and sweep rate dependent hysteresis loops expected for a single-molecule magnet.

Polymetallic clusters of paramagnetic transition metal ions can display the phenomenon of single-molecule magnetism if they combine a relatively large spin ground state with a large and negative zero-field splitting of that ground state.[1] This is a relatively rare combination which results in a significant barrier to thermally activated magnetization relaxation and thus far is most often found in complexes containing manganese.[2] Compared to other transition metals, clusters of manganese are often characterized by large spin ground states and this in conjunction with the presence of Jahn–Teller distorted Mn^{3+} ions makes manganese clusters ideal candidates for SMMs. The barrier to relaxation is given by $U = S^2|D|$ or $(S^2 - 1/4)\ |D|$ for integer and half-integer spins respectively, and intense effort is underway to maximise the magnitude of both parameters so that the proposed application of these materials may one day be realised.[3] To this end two successful, but somewhat opposing, synthetic strategies have been employed. The first is the use of rigid bridging ligands, *e.g.* cyanide, that impose the geometry on the resultant cluster[4] and the second is the use of flexible ligands that impose little or no geometry.[5] Both approaches have produced molecules with extremely large spin ground states – $S = 39/2$ for the former[6] and $S = 25$ and $S = 51/2$ for the latter[7] – but unfortunately these have not been coupled with large values of $|D|$. While the anisotropies of monomeric Mn^{3+} complexes can be relatively large ($|D| \sim 4\ cm^{-1}$), the magnitude of $|D|$ for polymetallic clusters of the same ion tends to be relatively small ($|D| < 0.50\ cm^{-1}$). For example, a [Mn18] SMM with one of the largest known ground state spin values, $S = 13$, has $D \approx -0.13\ cm^{-1}$,[8] whilst the smallest known SMM is a ferromagnetic dinuclear Mn^{3+} complex with a ground state of $S = 4$ and $D \approx -1.1\ cm^{-1}$.[9]

We have been exploring the reactivity of tripodal alcohols, such as 1,1,1-tris(hydroxymethyl)ethane (H_3thme) and 1,1,1-tris-(hydroxymethyl)propane (H_3tmp) in the synthesis of polynuclear 3d transition metal clusters, including manganese,[10] and have now extended this work to include the ligand *cis*,*cis*-1,3,5-cyclohexanetriol (H_3cht) – and herein report the synthesis, structure and magnetic properties of the first example of a trinuclear SMM and the first Mn SMM to contain only one Mn^{3+} ion.

Reaction of the dinuclear complex [$Mn_2O_2(bpy)_4](ClO_4)_3$ with one equivalent of H_3cht in MeCN produces a bright red solution from which orange crystals of [$Mn_3(Hcht)_2(bpy)_4](ClO_4)_3\cdot 1Et_2O\cdot 2MeCN$ (**1**$\cdot 1Et_2O\cdot 2MeCN$) are obtained upon diffusion of diethyl ether during one week. Complex **1**†‡ (Fig. 1) crystallises in the monoclinic space group *I*2/*m*. The metallic core of the complex comprises a linear [$Mn^{III}Mn^{II}_2O_4]^{3+}$ unit in which the central Mn ion (Mn1) is the sole Mn^{3+} ion. The metal ions are linked together by four μ_2-oxygens (O11 and symmetry

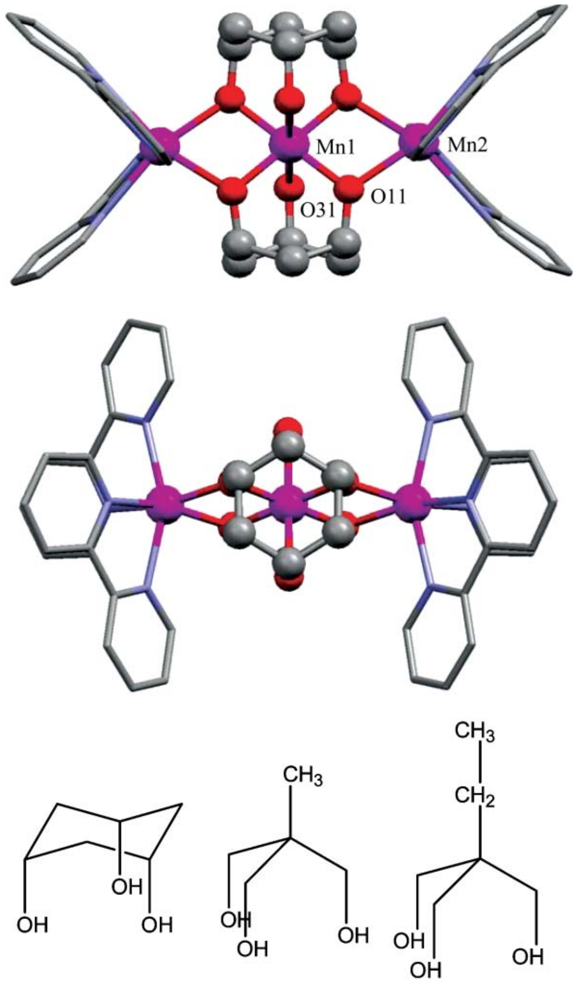

Fig. 1 The structure of complex **1** viewed parallel to the cyclohexane ring (top) and perpendicular to the cyclohexane ring (middle). Structures of the tripodal ligands H_3cht, H_3thme and H_3tmp (bottom).

---

*ebrechin@staffmail.ed.ac.uk

equivalents) from the two Hcht^{2-} ligands which sit directly, one above and one below, the [Mn$_3$] plane. The Mn–O–Mn bridging angle is 102°. The third oxygen atom (O31 and symmetry equivalent) of the ligand remains protonated (H-bonding the N-atom of the MeCN solvent molecule) and defines the direction of the Jahn–Teller axis of Mn1. The coordination of the peripheral Mn^{2+} ions is completed by two chelating bpy molecules. These Mn ions are in distinctly distorted octahedral geometries with *cis* angles in the range 72.30(16)–105.65(15)° and *trans* angles in the range 156.0(2)–158.17(14)°. The bond lengths for the Mn^{2+} ions lie in the range 2.142(4)–2.330(7) Å while the central Mn^{3+} ion has four short bonds of 1.898(3) Å in length and two longer bonds of 2.330(7) Å. The oxidation states of both were confirmed by bond valence sum (BVS) calculations which are summarised in Table 1. In the crystal the cations pack directly upon each other such that there are effectively 2D 'sheets' consisting of [Mn$_3$(Hcht)$_2$(bpy)$_4$]$^{3+}$ units with the ClO$_4^-$ ions between these sheets.

Variable temperature dc magnetic susceptibility data were collected on **1** (Fig. 2) in the temperature range 300–1.8 K in an applied field of 1 kG. The room temperature $\chi_M T$ value of approximately 12.3 cm^3 K mol^{-1} slowly increases upon cooling to approximately 75 K where it then increases rapidly to a maximum value of approximately 21.8 cm^3 K mol^{-1} at 3.3 K before dropping back to approximately 20.7 cm^3 K mol^{-1} at 1.8 K. The spin only (g = 2) value for a [Mn^{III}Mn$^{II}_2$] unit is approximately 12 cm^3 K mol^{-1}. This behaviour is indicative of ferromagnetic exchange between the metal centres resulting in an S = 7 ground state with the low temperature decrease assigned to zero-field splitting, Zeeman effects and/or intermolecular antiferromagnetic interactions.

In order to determine the spin ground state for complex **1**, magnetization data were collected in the ranges 10–70 kG and 1.8–6.0 K and these are plotted as reduced magnetization ($M/N\mu_B$) *vs.* H/T in Fig. 3. For a complex entirely populating the ground state and experiencing no zero-field splitting, the observed isofield lines should superimpose and saturate at a value ($M/N\mu_B$) equal to gS. The data were fitted by a matrix-diagonalization method to a model that assumes only the ground state is populated, includes axial zero-field splitting ($D\hat{S}_z^2$) and carries out a full powder average.

Table 1 BVS calculations for the metal ions in **1**

	Mn^{2+}	Mn^{3+}	Mn^{4+}	Assignment
Mn1	3.45	3.18	3.09	Mn^{3+}
Mn2	1.91	1.75	1.70	Mn^{2+}

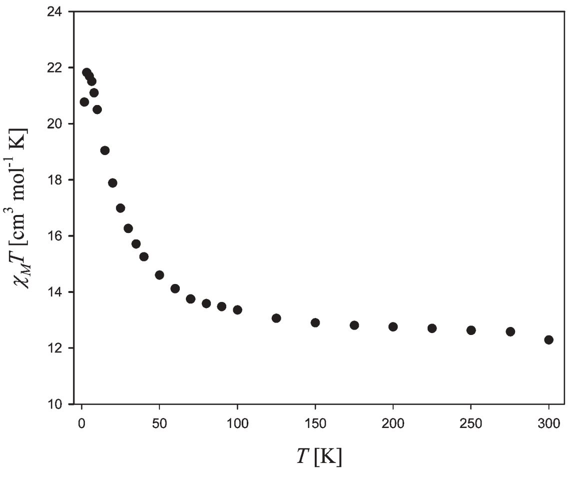

Fig. 2 Plot of $\chi_M T$ *vs.* T for complex **1** measured in the temperature range 1.8–300 K in a field of 1.0 kG.

The corresponding Hamiltonian is given by:

$$\mathcal{H} = D\hat{S}_z^2 + g\mu_B\mu_0\hat{S}_z H_z \quad (1)$$

where D is the axial anisotropy, μ_B is the Bohr magneton, μ_0 is the vacuum permeability, $\hat{S}_z$ is the easy-axis spin operator and H_z is the applied field. The best fit gave: S = 7, g = 1.87(3), D = −0.17 cm^{-1}.

Given the magnitude of S and sign of D, ac susceptibility studies were carried out in the 1.8–10.0 K range in a 3.5 G field oscillating at frequencies up to 1000 Hz. Frequency-dependent out-of-phase ac susceptibility signals were seen below approximately 3 K (but no peaks were observed) along with a concomitant decrease in the in-phase signal. The magnitude of the in-phase $\chi'_M T$ *vs.* T signals at >3 K supports the aforementioned spin ground state.

In order to probe the possible SMM behaviour further, single crystal hysteresis loop and relaxation measurements were performed using a micro-SQUID setup.[11] Fig. 4 presents typical magnetization (M) *vs.* applied dc field measurements at a field sweep rate of 0.002 T/s. A hysteresis loop was observed, whose coercivity was strongly temperature and time dependent, increasing with decreasing temperature and increasing field sweep rate, as expected for the superparamagnetic-like behaviour of an SMM, with a blocking temperature (T_B) of ~0.5 K. The hysteresis loops also show the step-like features indicative of quantum tunnelling of magnetization (QTM) between the energy states of the molecule.

In conclusion, use of the tripodal ligand H$_3$cht has produced a trinuclear manganese complex containing one Mn^{3+} ion and two Mn^{2+} ions that are coupled ferromagnetically to give a spin ground state of S = 7. The observed anisotropy is rather small, D = −0.17 cm^{-1}, and considerably smaller than that seen for mononuclear Mn^{3+} complexes. Nevertheless complex **1** does

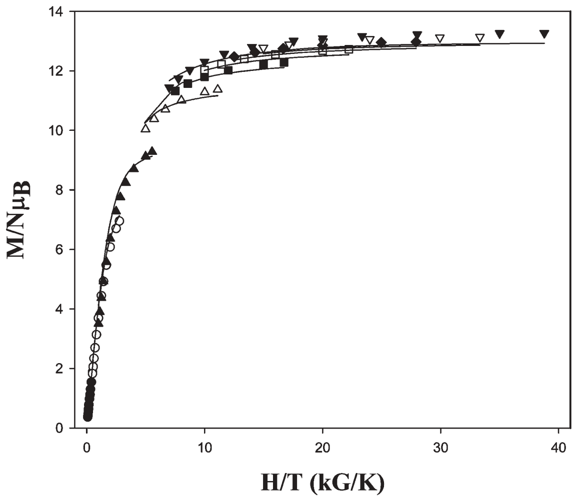

Fig. 3 Plot of reduced magnetization ($M/N\mu_B$) *vs.* H/T for complex **1**. The solid lines are fits of the data to an S = 7 state with g = 1.87(3) and D = −0.17 cm^{-1} in a field range of 10–70 kG.

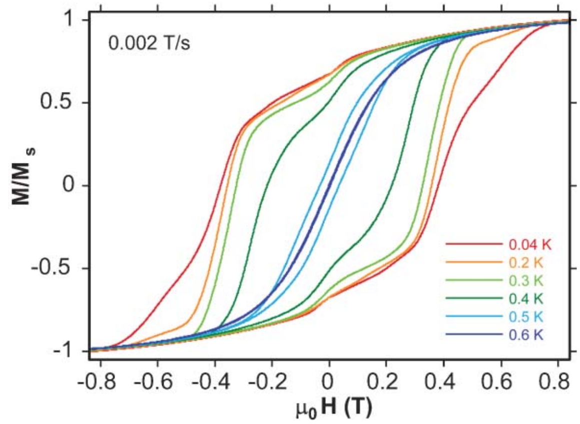

Fig. 4 Magnetization (*M*) *vs.* dc field hysteresis loops for **1** at a field scan rate of 0.002 T/s in the temperature range 0.6–0.04 K.

display the temperature and sweep rate dependent hysteresis loops diagnostic of an SMM and is thus the first example of a trinuclear SMM, the first example of a Mn SMM containing only one Mn^{3+} ion, the second smallest SMM reported and one of the smallest clusters to show QTM. Given the previous success of other related tripodal organic ligands in the formation of novel SMMs, the use of the ligand H_3cht promises much.

The authors would like to acknowledge Lloyd's of London Tercentenary Foundation, the EPSRC (UK), the Leverhulme Trust (UK) and the National Science Foundation (USA).

Richard T. W. Scott,[a] Simon Parsons,[a] Muralee Murugesu,[b] Wolfgang Wernsdorfer,[c] George Christou[b] and Euan K. Brechin*[a]
[a]*School of Chemistry, The University of Edinburgh, West Mains Road, Edinburgh, UK EH9 3JJ. E-mail: ebrechin@staffmail.ed.ac.uk; Tel: +44 (0)131-650-7545*
[b]*Department of Chemistry, University of Florida, Gainesville, FL 32611-7200, USA*
[c]*Laboratoire Louis Néel-CNRS, 38042, Grenoble, Cedex 9, France*

Notes and references

† Complex **1** analysed satisfactorily (C, H, N) as **1**·0.5 MeCN. Crystals were kept in contact with mother liquor to avoid solvent loss and were crystallographically identified as **1**·Et_2O·2MeCN.

‡ Diffraction data were collected with Mo-Kα X-radiation (λ = 0.71073 Å) on a Bruker Smart APEX diffractometer equipped with an Oxford Cryosystems low-temperature device operating at 150 K. An absorption correction was applied using the program SADABS;[12] the structure was solved using Patterson methods (DIRDIF)[13] and refined by full-matrix least squares against F^2 (Shelxtl)[12] using all unique data. Crystal Data: $C_{60}H_{68}Mn_3Cl_3N_{10}O_{19}$, M = 1504.41, orange blocks, monoclinic, *I*2/*m*, a = 11.919(2), b = 22.044(4), c = 13.385(2) Å, β = 96.863(4)°, V = 3491.6(10) $Å^3$, 14880 reflections measured, of which 3915 were independent, θ_{max} = 27.04°, 901 parameters and 13 restraints, R = 0.0953 [based on $F > 4\sigma(F)$], R_w = 0.2653 (based on F^2 and all data). CCDC 263449. See http://www.rsc.org/suppdata/cc/b5/b501504a/ for crystallographic data in CIF or other electronic format.

1 R. Sessoli, H.-L. Tsai, A. R. Schake, S. Wang, J. B. Vincent, K. Folting, D. Gatteschi, G. Christou and D. N. Hendrickson, *J. Am. Chem. Soc.*, 1993, **115**, 1804.
2 D. N. Hendrickson, G. Christou, H. Ishimoto, J. Yoo, E. K. Brechin, A. Yamaguchi, E. M. Rumberger, S. M. J. Aubin, Z. Sun and G. Aromí, *Mol. Cryst. Liq. Cryst.*, 2002, **376**, 301.
3 M. Leuenberger and D. Loss, *Nature*, 2001, **410**, 789; R. Sessoli, D. Gatteschi, A. Caneschi and M. A. Novak, *Nature*, 1993, **365**, 141.
4 See for example V. Marvaud, C. Decroix, A. Scuiller, C. Guyard-Duhayon, J. Vaissermann, F. Gonnet and M. Verdaguer, *Chem. Eur. J.*, 2003, **9**, 1677; A. Scuiller, T. Mallah, M. Verdaguer, A. Nivorozkhin, J. L. Thiolence and P. Veillet, *New J. Chem.*, 1996, **20**, 1; J. J. Sokol, A. G. Hee and J. R. Long, *J. Am. Chem. Soc.*, 2002, **124**, 7656; H. J. Choi, J. J. Sokol and J. R. Long, *Inorg. Chem.*, 2004, **43**, 1606; C. P. Berlinguette, D. Vaughn, C. Cañada-Vilalta, J. R. Galan-Mascaros and K. M. Dunbar, *Angew. Chem., Int. Ed.*, 2003, **42**, 1523.
5 See for example D. N. Hendrickson, G. Christou, H. Ishimoto, J. Yoo, E. K. Brechin, A. Yamaguchi, E. M. Rumberger, S. M. J. Aubin, Z. Sun and G. Aromí, *Polyhedron*, 2001, **20**, 1479; C. J. Milios, C. P. Raptopoulou, A. Terzis, F. Lloret, R. Vicente, S. P. Perlepes and A. Escuer, *Angew. Chem., Int. Ed.*, 2003, **43**, 210; L. M. Wittick, K. S. Murray, B. Moubaraki, S. R. Batten, L. Spiccia and K. J. Berry, *Dalton Trans.*, 2004, 1003; C. Cadiou, M. Murrie, C. Paulsen, V. Villar, W. Wernsdorfer and R. E. P. Winpenny, *Chem. Commun.*, 2001, 2666.
6 Z. J. Zhong, H. Seino, Y. Mizobe, M. Hidai, A. Fujishima, S. Ohkoshi and K. Hashimoto, *J. Am. Chem. Soc.*, 2000, **122**, 2952.
7 M. Murugesu, M. Habrych, W. Wernsdorfer, K. A. Abboud and G. Christou, *J. Am. Chem. Soc.*, 2004, **126**, 4766; D. M. Low, L. F. Jones, A. Bell, E. K. Brechin, T. Mallah, E. Riviere, S. J. Teat and E. J. L. McInnes, *Angew. Chem., Int. Ed.*, 2003, **42**, 3781; G. Rajaraman, J. Cano, E. K. Brechin and E. J. L. McInnes, *Chem. Commun.*, 2004, 1476.
8 E. K. Brechin, E. C. Sañudo, W. Wernsdorfer, C. Boskovic, J. Yoo, D. N. Hendrickson, A. Yamaguchi, H. Ishimoto, T. E. Concolino, A. L. Rheingold and G. Christou, *Inorg. Chem.*, 2005, **44**, 502.
9 H. Miyasaka, R. Clérac, W. Wernsdorfer, L. Lecren, C. Bonhomme, K. Sugiura and M. Yamashita, *Angew. Chem., Int. Ed.*, 2004, **43**, 2801.
10 G. Rajaraman, M. Murugesu, M. Soler, W. Wernsdorfer, M. Helliwell, S. J. Teat, G. Christou and E. K. Brechin, *J. Am. Chem. Soc.*, 2004, **126**, 15445.
11 W. Wernsdorfer, *Adv. Chem. Phys.*, 2001, **118**, 99.
12 G. M. Sheldrick, *SHELXL-97*, University of Gottingen, Germany, 1997.
13 P. T. Beurskens, G. Beurskens, W. P. Bosman, R. de Gelder, S. Garcia-Granda, R. O. Gould, R. Israel and J. M. M. Smits, *The DIRDIF96 Program System, Technical Report of the Crystallography Laboratory*, University of Nijmegen, The Netherlands, 1996.